Small scale topographical influences on precipitation

By PER B. STOREBØ, *Norwegian Defence Research Establishment, N-2007 Kjeller, Norway*

(Manuscript received September 23, 1974; in final form April 24, 1975)

ABSTRACT

Small clouds may form above small hills when moist air blows over a landscape. Removal of droplets from these clouds by raindrops from above is the only suggested mechanism which directly links rainfall patterns to small scale topographical features. This mechanism is examined theoretically, and results from a series of computations are presented. The properties of condensation nuclei are found to be of minor importance for the condensation development, because the activation of nuclei dwindles off when enough droplets have been formed, and because a droplet assembly is an instable phenomenon. Additional rainfall over small hills is found to be sufficiently large to explain observed influences of small scale terrain features on precipitation in Scandinavia.

1. Introduction

The influence on weather of mountain ridges has long since been recognized. The role of smaller scale landscape features has scarcely been mentioned for anything but increased surface friction, before Bergeron (1949) pointed out certain systematic precipitation patterns, which appeared to be linked to surface topography of very limited height. An extensive search for small scale precipitation effects was later on carried out by him in the Uppsala region in Sweden (Bergeron, 1960, 1967–73), and the results indicate that relatively low hills, of the order of 50 m above the general level, may cause an increase of up to 25, sometimes even 50, per cent in rainfall amounts, noticeably when extensive precipitation areas pass over the area.

Bergeron's explanation (1950, 1965) is that the small scale terrain features cause formation of low level feeder clouds, with droplets too small for independent rain formation, but with droplets large enough to be removed by precipitation falling from above.

The same mechanism was later used by the author (Storebø, 1968) to explain the deposition pattern of nuclear bomb debris in western Norway.

Storebø & Dingle (1974) have worked out a procedure for quantitative computation of growth and removal of droplet aerosols under steady state conditions. A slightly improved version is used in this paper to examine the Bergeron theory.

2. Method of calculation

An aerosol element following a certain course in a vertical plane is studied by computation, and the results regarding droplet formation and removal are examined for different condensation nucleus configurations, courses, wind speeds and precipitation amounts.

The effects of electrolytic solutes upon the formation of the low level cloud are computed by means of the formulation and tables of Low (1969).

The condensation nuclei are assumed to be made up of the hygroscopic ammonium sulfate together with an inactive component having density and specific heat equal to those for graphite (Hodgman, 1961). Log-normal size distributions are used, and thirty size classes are specified in the radius range between 1.5×10^{-6} and 1.33×10^{-3} cm, in such a way that dry particle volume is doubled from one class to the next. No particles are considered to exist outside the defined range.

When condensation occurs, the heat of condensation is supplied to the droplets. The air is affected secondarily by heat conduction from the assembly of droplets. Another heat source for the air is dissipation of kinetic energy from falling drops. The condensed water is removed from the air, and a record is kept of the vapour concentration in the air.

When vertical displacements occur along the path, air pressure is assumed to follow ICAO's standard atmosphere. Two path configurations are used. One is a model from which conclusions regarding low hills can be drawn. The other involves larger total ascent corresponding to a rougher terrain. It is the paths which are defined, however, and related terrain features can be vaguely inferred only.

Within a time step each droplet class is treated without reference to other classes. The interclass influence is brought about by the changes occurring in the ambient air temperature and vapour concentration from one time step to the next. The volume of the liquid water is a small fraction of the total volume. The volume of the droplets and the deviating state parameters in their surrounding shells can therefore be disregarded when ambient values are computed.

A droplet of radius r in an environment with a vapour concentration ϱ_a changes in size due to vapour diffusion under quasi-stationary conditions

$$\frac{dm}{dt} = 4\pi r D(\varrho_a - \varrho_d)\,\beta_D\, V = B(\varrho_a - \varrho_d) \tag{1}$$

where m is droplet mass and t is time, D is the diffusion coefficient for vapour in air, β_D is the Fuchs correction factor for condensation on small drops (Fuchs, 1959), V is a tabulated ventilation factor (Squires, 1952), and ϱ_d is the vapour concentration corresponding to the droplet saturation humidity, i.e. that leading to no mass change for the droplet.

The droplet saturation humidity may be written

$$\varrho_d = \varrho_s(T)\cdot a(\mu)\cdot \exp\,(2M\sigma/\varrho RTr) \tag{2}$$

where $\varrho_s(T)$ is the saturation concentration over a flat surface of pure water at temperature T, in principle defined by the vapour pressure formula of Goff & Gratch (1946); a is the hygroscopic activity defined as the ratio between the saturation concentration over the solution and that over pure water, and therefore dependent on the molality μ, M is the molecular weight of the vapour, σ and ϱ are surface tension and density of the solution, and R the gas constant.

For a time step in the computation, ϱ_d will be known at the start. Condensation or evaporation leads to changes in droplet temperature, molality and radius. In order to integrate (1) it is necessary to express ϱ_d as a function of the water mass m being condensed.

Because time steps are short, it should be sufficient to consider first order changes only. Derivation of (2) then leads to

$$\frac{d\varrho_d}{dm} = \varrho_d\left[\frac{1}{\varrho_s}\frac{d\varrho_s}{dT}\frac{dT}{dm} + \frac{1}{a}\frac{da}{d\mu}\frac{d\mu}{dm} + \frac{d(2M\sigma/\varrho RTr)}{dr}\frac{dr}{dm}\right] \tag{3}$$

The first term, which depends on the droplet temperature, is the most important one. It is further the only term for which an expression cannot readily be found.

The method developed by Storebø & Dingle (1974) is used in order to carry through the calculation. If a vapour mass m is condensed during the time step, a fictitious temperature rise ΔT may be defined by supplying the heat of condensation to the droplet. After considering heat conduction between droplet and air, a mean temperature rise $\Delta\bar{T}$ is found. It is assumed that when the rate of condensation is quasi-steady, the ratio $\nu = \Delta\bar{T}/\Delta T$ should be fairly conservative from one step to the next.

It is obviously the mean temperature rise which is of interest in equation (3). Assuming that ν from the previous step can be used, the first term may be treated as a constant and the equation can be integrated.

$$\varrho_d = \varrho_d' + \left[\left(\frac{d\varrho_d}{dT}\right)_0 \frac{L + c_p(T_a - T_0) - 2\sigma_0/r_0}{C_0}\,\nu - \frac{\varrho_d'}{a_0}\left(\frac{da}{d\mu}\right)_0 \frac{\mu_0}{m_0} - \varrho_d' \frac{\sigma_0 M}{2\pi r_0^4 RT\varrho_0}\right] \times m = \varrho_d' + \gamma m \tag{4}$$

ϱ_d' is the saturation concentration at the beginning of the step, L is the latent heat of condensation, c_p the specific heat of water vapour, T_a is the ambient air temperature, σ droplet surface energy and C the droplet heat capacity. Indexes o indicate the values of the pertinent quantities at the beginning of the step. The factor γ consequently varies from one drop size to another and from one step to the next.

After inserting (4) into (1)

$$\frac{dm}{dt} = B(\varrho_a - \varrho_d' - \gamma m) \qquad (5)$$

with the solution for Δm over the time interval Δt

$$\Delta m = \frac{\varrho_a - \varrho_d}{\gamma}(1 - e^{-\gamma B \Delta t}) \qquad (5)$$

In accordance with Bergeron's theory the increased rainfall due to impact-collection of the droplets by falling raindrops is computed. The raindrop number in classes with different sizes is computed by means of the formulation of Marshall and Palmer (1948). The removal of the cloud droplets by the raindrop population is based on collision efficiency values adapted from Mason (1971). Limitations and approximations are discussed by Storebø & Dingle (1974).

3. General description of the results

The computational model groups the nuclei into size classes, which is at variance with the continuous distributions found in nature. An immediate result is uneven variations in the development, caused by class boundaries. Serious distortion may occur close to the boundary between nuclei activated and not activated by the humidity course. Some of the results indicate that activation of large class groups as units influences the further development in such a way that some conclusions are imperiled.

Two different course profiles and consecutive computations with gradual change in one parameter are used in order to overcome the defaults. The conclusions drawn from the whole material should therefore have a more general validity.

A computation starts with an assembly of dry nuclei in saturated air at 288.16 K. This aerosol adjusts internally its humidity and temperature conditions over 200 s, and an initial droplet aerosol is thus produced. Both courses start with a 25 m ascent over a 5 km distance to simulate air approaching and entering an area with significant topographical features. For the low hills course the 25 m represent a general level for the low-lying part of the course. A real path in the air is certainly more irregular. Furthermore no turbulent exchange, horizontal divergence, vertical layer structure or time variations are considered. Conclusions are drawn with these limitations in mind.

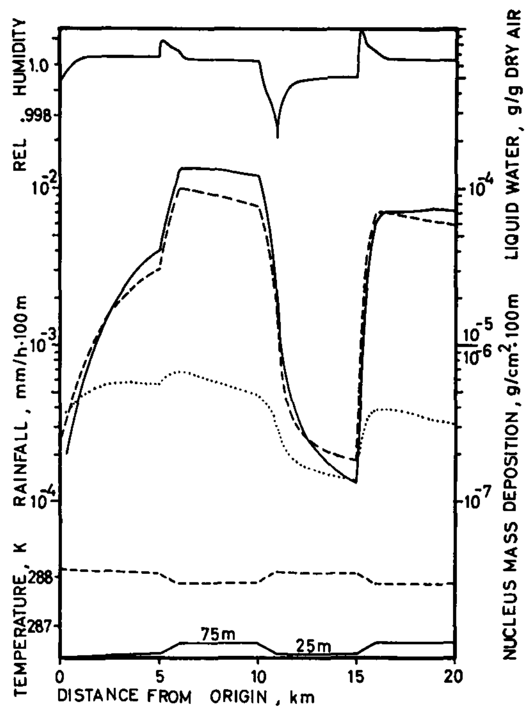

Fig. 1. State and precipitation parameters along the low-hills course. Additional rainfall is shown by the solid, liquid water by the broken and nucleus mass deposition by the dotted curve in the middle part of the diagram. Air temperature is shown by the broken curve just above the course profile in the lower part. The particle concentration at start is 3 770 per cm³ with a geometric mass mean radius 4.65×10^{-5} cm, altogether 8.5×10^{-11} g/cm³. Hygroscopic/neutral mass is 1/5. The horizontal wind speed along the course is 5 m/s and the rainfall from above 1 mm/h.

During the calculations the droplet development and the removal are studied along the course together with state parameters for the air. Removed liquid water and nucleus mass are presented as the additional precipitation and deposition from an air layer of 100 m original depth. The depth is locally modified in order to keep a constant mass of dry air in the layer.

The results presented in Fig. 1 are typical for

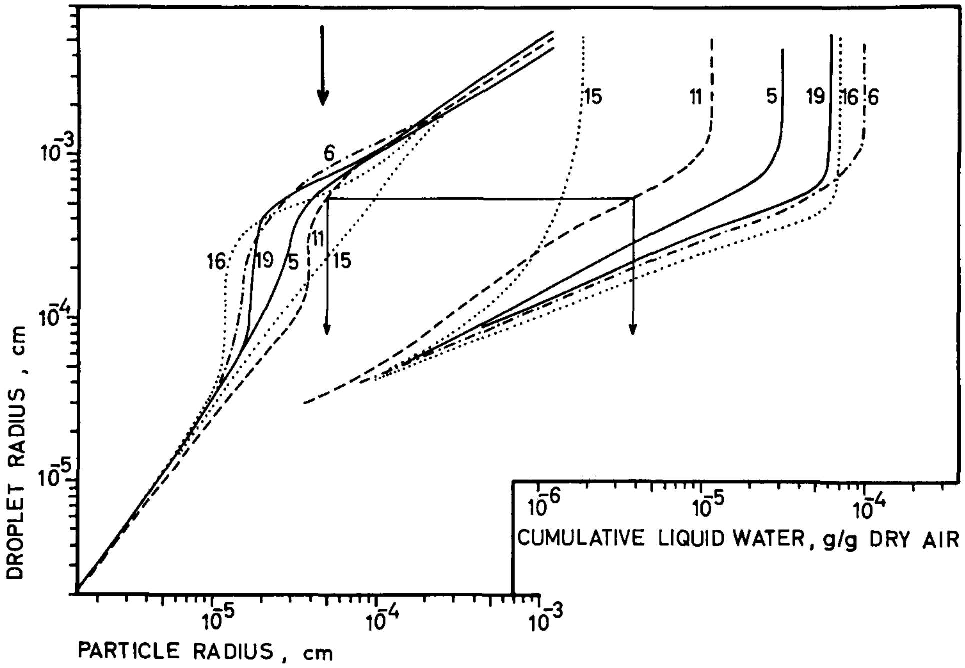

Fig. 2. Droplet sizes and liquid water distribution at specified points as a function of the dry nucleus size. Distances from the origin in km are shown by the numbers associated with the curves. The conditions are those described in Fig. 1. The droplet distributions in the left-hand part correspond to the liquid water contents in the right-hand part. The angled thin line with arrows shows how the nucleus particle size is linked to the liquid water content. The thick arrow indicates the geometric mass mean radius for the nuclei.

the low hills course. The total liquid water on the particles shows a development very similar to the rainfall component caused by droplet removal, and the curves are further sharply defined by the elevations in the course. For the case shown rainfall from a 1 000 m column would be necessary in order to increase the amount over the hill by 10 per cent.

Over the descent towards the lower level a rapid evaporation takes place. The removal of water from the air over the first hill is great enough to bring the relative humidity well below saturation over the low part of the course.

Evaporation of or condensation on raindrops may increase or decrease the difference between low and high land, depending on the assumptions regarding raindrop temperature. The spatial structure of the precipitation system should be taken into account if this question is to be considered. It is clearly outside the scope of a model where conditions along a specified path only are examined.

The effect of the hills is pronounced also in the deposition of nucleus material. A prominent feature is a high deposition very early in the course. The initial nucleus distribution apparently contains some material which is easily accessible by way of rain removal.

Fig. 2 shows droplet and liquid water distribution at different points along the course. The distributions are shown as function of nucleus or particle size in the original dry aerosol. At 5 km from the origin, after a slow 25 m ascent, condensation has produced a definite hump in the distribution, and most of the water is associated with droplets on the upper part of the hump. If exception is taken to the effect of class boundaries, the most rapid rise in droplet size with particle size coincides with the boundary between inactivated nuclei, i.e. those in stable equilibrium with their saturation humidity, and activated nuclei, i.e. those in instable equilibrium with their saturation humidity.

At 6 km from the origin, after an additional

50 m ascent, causing a peak in the relative humidity course, the boundary for activated nuclei is shifted towards smaller particles, while the bulk of the water is associated with larger droplets than before.

The next curve, at 11 km from the origin shows the situation just after the descent from the first hill. The boundary for the activated nuclei is again shifted towards larger nuclei. The inactivated nuclei are smaller than ever before in accordance with the reduced humidity, but the droplets associated with the largest nuclei are surprisingly enough larger than before. Closer inspection reveals that even they are evaporating at this stage, but the response is quite small.

At 15 km from the origin, after 4 km horizontal course, an adjustment has taken place. The relative humidity has increased due to evaporation from droplets in the middle part of the size distribution, while the smaller and the very largest droplets have grown. The result is that the liquid water is now spread over a very wide droplet size range.

At 16 km from the origin, at the top of the second hill, a new spell of condensation has shifted back the activation boundary towards smaller nuclei than ever before. The reason is evidently that so many large nuclei are removed that the rest cannot cope with the demand for condensation. The relative humidity rises and smaller nuclei are activated. However, the droplet size distribution still displays a slight hump at the position for the 15 km hump. The condensation history therefore is of significance for the droplet distribution.

The last distribution shown, at 19 km from the origin, corresponds to the small peak in precipitation after a 3 km horizontal course along the second hill. The activation boundary has again crept up towards larger sizes and the main part of the droplets above have increased their size. The reason for the rainfall peak must be that the conditions for water removal by rain are optimized in the adjusted distribution. The liquid water curves clearly show that even if the aerosol contains less water than at 16 km, it is associated with larger droplets which should be more easily removed.

The developments of the droplet sizes in the activation boundary region give rise to some reflective thoughts upon the meaning of activation. The course between 16 and 19 km is

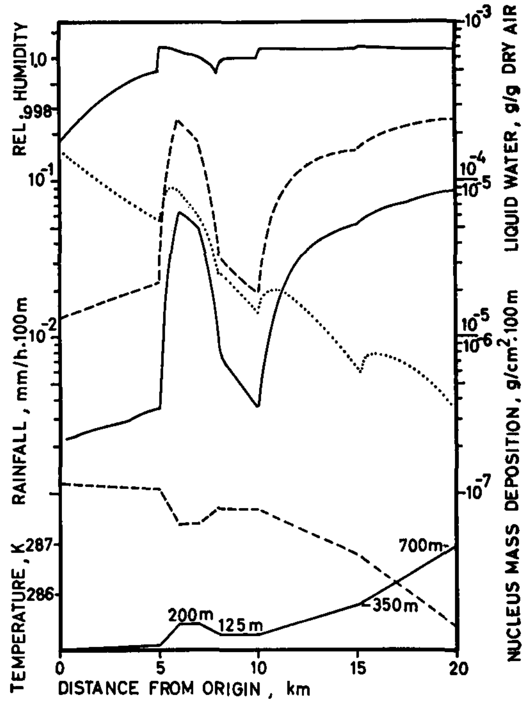

Fig. 3. State and precipitation parameters along the rough terrain course. The lay-out of the diagram is similar to Fig. 1. The particle concentration at start is 6 010 per cm^3 with a geometric mass mean radius 10^{-4} cm, altogether 1.2×10^{-9} g/cm^3. Hygroscopic/neutral mass is 1/5. The wind speed is 2 m/s and the rainfall from above 2.5 mm/h.

horizontal, the relative humidity is above saturation and there is only inconsiderable energy transfer out of the droplet/air system due to droplet removal. Yet part of the activated nuclei loose their water and become unactivated.

The reason is that instable equilibrium is to delicate to exist within a droplet distribution. All the distributions shown in Fig. 2 have one thing in common: Droplet saturation humidities decrease with increasing size. Consequently, the immediate air humidity adjusts itself somewhere within the range of the droplet saturation humidities when the system is not affected by any outside influence. Because the equilibrium for each droplet is instable, those requiring a higher humidity than that present evaporate, while the others grow. A steady shift upwards in the critical droplet size should be expected, with the ultimate results that all the water, apart from that found on inactivated

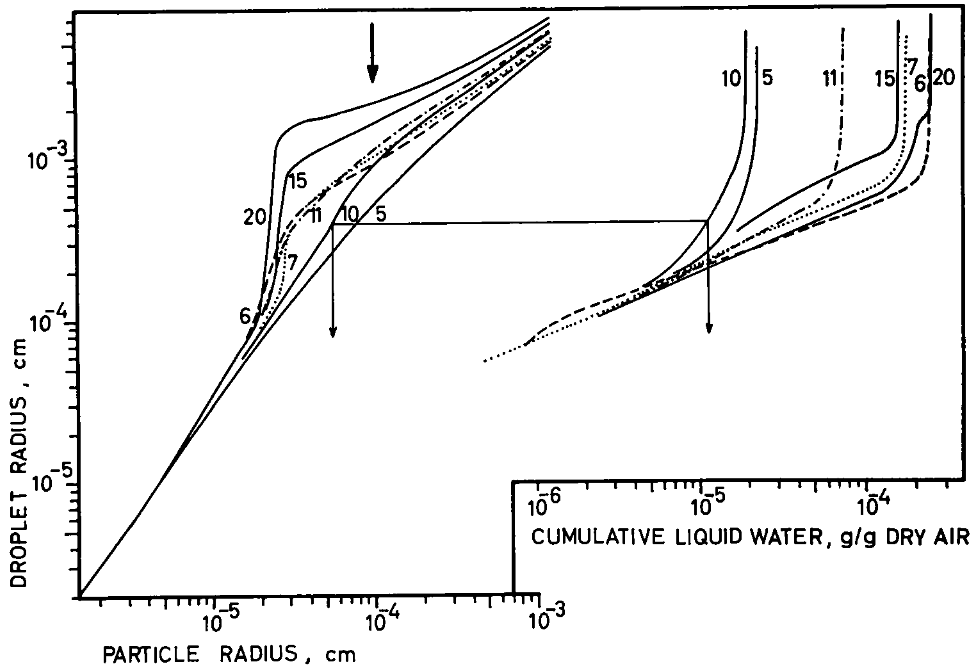

Fig. 4. Droplet sizes and liquid water distribution at specified points as a function of the dry nucleus size. The conditions are those described in Fig. 3, and the lay-out is similar to Fig. 2.

nuclei, should be associated with the most powerful nucleus present. This then should be the only possible stable equilibrium of a nucleus/droplet distribution.

A general conclusion from the computation presented is that inactivated droplets respond most easily to rapid changes in humidity conditions. If necessary the largest ones are activated to cope with the condensation demand. A gradual readjustment then take place afterwards, and during the adjustment period the initial change propagates towards larger sizes.

Fig. 3 presents results from a rougher course and with a much larger mean aerosol particle size. The hygroscopic power of these particles is so great that the air humidity is below saturation even after 25 m ascent, but the relative humidity amplitudes are otherwise less than for the previous case. The nucleus distribution is apparently better suited to cope with changing conditions, but at the same time the removal of nucleus mass is high everywhere on the course.

The agreement between liquid water content and rainfall removal is good, and the course profile is reflected in both quantities. It is interesting to note how well the increased rate of ascent at 15 km comes out in the precipitation curve, and especially in the nucleus mass deposition curve. Apart from small adjustments when rate of ascents are changed, the temperature adheres closely to an inverse course profile.

The 200 m high elevation between 6 and 7 km from the origin is sharply reflected in the extra rainfall caused by droplet removal. The fraction removed is quite large, since a similar level of extra rainfall is later found only after a total ascent of some 400 m. For liquid water the level at the hill top is reached at the end of the course at 700 m height.

The maximum rainfall over the hill corresponds to 2.5 per cent of the rain from above per 100 m air layer. The rates of decrease along the horizontal pieces of the course are high, but for a quantitative comparison with Fig. 1 the lower wind speed and the greater ascent in the present case should be considered.

The nucleus mass deposition is more clearly shifted towards the windward side of the profile than earlier. This shift is a general feature for removal, and it is most emphasized for slow ascent and heavy rainfall from above.

Droplet and liquid water distributions relat-

Table 1. *Particle composition effects*

Low hills: particle number 3 770 per cm^3; particle geometric mass mean radius 2.15×10^{-5} cm

Hygroscopic/ neutral mass ratio	Liquid water g/g dry air		Final fraction left of nuclei	
	Initial	Final	Mass	Number
1	1.28×10^{-6}	5.81×10^{-5}	0.50	0.98
5	1.85×10^{-6}	5.85×10^{-5}	0.49	0.98

ing to Fig. 3 are shown in Fig. 4. After an ascent of 25 m, 5 km from the origin, the air is still not saturated, and the droplets, especially those formed on the larger nuclei, are smaller than those in Fig. 2. The reason should be sought in the nucleus distribution itself, since it is opposite to the effect expected for equal distributions having different time available for adjustment. The increase with nucleus size is gradual over the whole distribution, and the liquid water is spread over a wide size range. Less liquid water is present than on Fig. 2. This is partly due to increased removal caused by heavier rainfall from above together with increased exposure time because of lower wind speed.

At 6 km, after additional rise of 175 m, a distinct hump appears in the distribution and the liquid water is associated with a narrow droplet range.

The next distribution is for 7 km, after 1 km horizontal course. The hump has shifted towards larger nuclei, and the smaller droplets have decreased in size, while the larger ones have increased. This is the same effect as that observed for the first case: The smaller droplets respond rapidly to humidity changes, but when the system is left without outside influence, internal adjustment takes place.

At 10 km from the origin the air has experienced a descent of 75 m followed by a horizontal course of 2 km. The middle-size nuclei have lost considerable amounts of water, while the largest ones have grown. The result is that the liquid water is once more associated with a wide droplet range.

The main ascent starts at 10 km and a rapid increase in the rainfall occurs. The droplet distribution at 11 km shows that the middle-size nuclei have accumulated water and are growing together with the larger ones.

The droplet distributions at 15 and 20 km from the origin, after continued rise through 350 to 700 m height, show increased size of the largest droplets and a steady shift in the activation boundary towards smaller nuclei. The liquid water is associated with a narrow size range of droplets, although a peculiar twist occurs in the 20 km distribution curve, almost certainly a numerical effect caused by class boundaries.

As far as they are relevant, the conclusions drawn during the discussion of the low hills course appear to be valid also for the more rough course.

4. Influence of individual parameters

In order to study the influence of different parameters, series of computations were carried through. Everything except one parameter remains unchanged throughout each series. Only the parameters considered to be the most important ones are studied.

4.1. *Nucleus composition*

The results presented in Table 1 refer to two widely different particle compositions, but the numbers shown are about the same. Extra precipitation and deposition along the course show similar small differences. The composition appears in this case not to have had any noticeable effect.

One might, however, hesitate to draw a general conclusion based on such a limited material. Another active agent or a different configuration of other parameters might lead to a higher sensitivity relative to nucleus composition.

On the other hand the liquid water with which activated nuclei are associated, is normally large enough to give a very low molality

Table 2. *Particle size effects*

Low hills: particle number 3 770 per cm^3

Particle geometric mass mean radius, cm	Liquid water g/g dry air		Final fraction left of nuclei	
	Initial	Final	Mass	Number
10^{-5}	6.19×10^{-8}	5.46×10^{-5}	0.62	0.98
4.65×10^{-5}	2.67×10^{-6}	5.84×10^{-5}	0.45	0.98
10^{-4}	1.05×10^{-5}	5.93×10^{-5}	0.41	0.97

for the solution, and therefore a negligible effect of the composition. During the activation phase the composition is important under otherwise equal conditions. Afterwards, the relative humidity adjusts itself to a value dependent on the whole nucleus assembly, and this may counteract any strong influence of the nucleus composition.

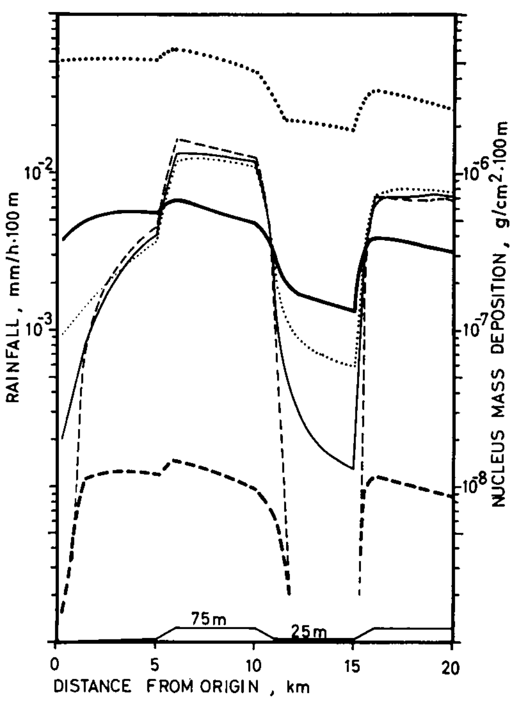

Fig. 5. Additional precipitation and deposition for different dry particle sizes. The course profile is shown at the bottom of the diagram. Additional rainfall along the course is indicated by thin curves, deposition of nucleus mass by thick curves. Broken curves are for a geometric mass mean radius 10^{-5} cm, solid for 4.65×10^{-5} and dotted for 10^{-4} cm, corresponding mass 2.5×10^{-12}, 8.64×10^{-11} and 7.53×10^{-10} g/cm^3. Hygroscopic/neutral mass is 1/5. The particle concentration is 3 770 per cm^3, rainfall from above 1 mm/h and wind speed 5 m/s.

4.2. *Nucleus size*

Results from computations with different geometric means of nucleus radii (mass weighted) are shown in Table 2 and Fig. 5.

An increase of the mean radius results in more large nuclei compared to smaller ones. It is not obvious that this results in more activated particles, since the whole assembly plays a role in determining humidity conditions during the condensation.

The small differences in precipitation over the elevations are not considered significant; they may be caused by class boundaries influencing droplet sizes. And smaller droplets will automatically result in less removal.

The differences over the lower part of the course are considerable. The more small nuclei there are, the faster is the evaporation, and the less is the precipitation. The behaviour is in general agreement with the earlier observation that small droplets react rapidly to changes in state, but the development may also be influenced by the differences in droplet removal over the first elevation, which should emphasize the effect.

The level of mass deposition is essentially determined by the amount present, and the amount increases with size when the number is constant. Further, when the geometric mean radius increases, a larger fraction of the mass is associated with the nuclei removed. The final fraction left is for this reason considerably lower for the largest than for the smallest radius in Table 2. It is interesting to note, however, that the nucleus number is not much reduced, even for the largest removal.

Table 3. *Particle number effects*

Low hills: particle geometric mass mean radius 4.65×10^{-5} cm. Rough terrain: particle geometric mass mean radius 10^{-4} cm

Initial particle number per cm^3	Liquid water g/g dry air		Final fraction left of nuclei	
	Initial	Final	Mass	Number
Low hills				
535	6.46×10^{-7}	5.46×10^{-5}	0.33	0.90
1 000	1.06×10^{-6}	5.63×10^{-5}	0.37	0.93
3 770	2.67×10^{-6}	5.84×10^{-5}	0.45	0.98
Rough terrain				
1 200	5.45×10^{-6}	4.45×10^{-4}	0.06	0.74
2 410	8.09×10^{-6}	4.61×10^{-4}	0.09	0.83
6 010	1.33×10^{-5}	4.84×10^{-4}	0.13	0.90

4.3. *Nucleus concentration*

Results from two series of computations with systematic change in number of nuclei per cm^3 are presented in Table 3 and Figs. 6 and 7. The general impression from both diagrams is less precipitation over the hills with increasing particle concentration. The tendency may be reversed over the lower parts of the course, but Table 3 indicates that invariably more liquid water is present in the air finally, when the nucleus number is highest.

The differences in rainfall pattern are surprisingly small. In Fig. 6 they are even smaller over the hills than in the previous figure, and nucleus class boundaries could have some influence.

The final nucleus masses and numbers left in the air clearly show that nuclei of smaller size are removed when the nucleus number is small than when it is great. The boundary between activated and non-activated nuclei is therefore shifted downwards with decreased concentration. This have a profound influence on nucleus mass deposition, but need not matter much for the precipitation development.

Fig. 7 exhibits features similar to those discussed. The nucleus distributions are different and the new course a more violent one. Only little more precipitation is found over the first hill for the lowest than for the highest nucleus number. It is more surprising that the difference is kept up over the whole ascent from 125 to 700 m, although a tendency towards equalization is present at the top. The highest nucleus number

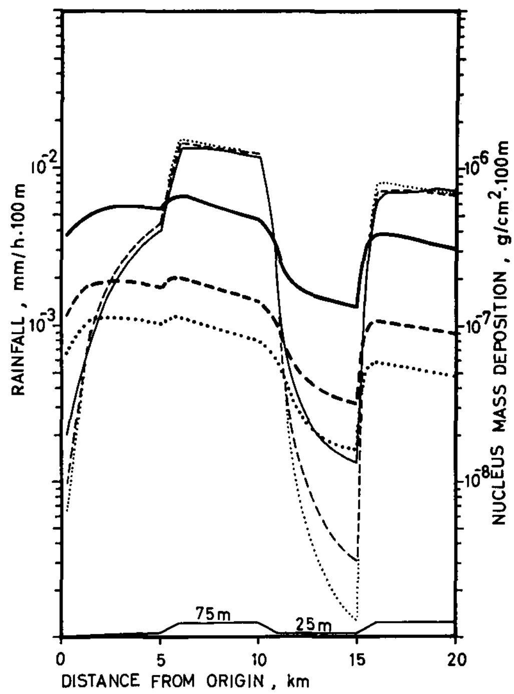

Fig. 6. Additional precipitation and deposition for different dry particle concentrations. The course profile is shown at the bottom of the diagram. Additional rainfall along the course is indicated by thin curves, deposition of nucleus mass by thick curves. Dotted curves are for 535 particles per cm^3, broken for 1 000 per cm^3 and solid for 3 770 per cm^3, corresponding to 1.2×10^{-11}, 2.24×10^{-11} and 8.46×10^{-11} g/cm^3 respectively. Hygroscopic/neutral mass is 1/5. The geometric mass mean radius is 4.65×10^{-5} cm, rainfall from above is 1 mm/h and wind speed 5 m/s.

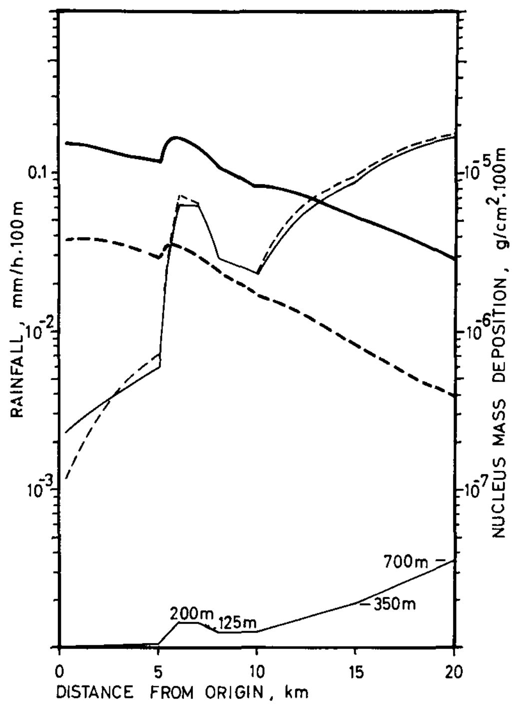

Fig. 7. Additional precipitation and deposition for different dry particle concentrations. The course profile is shown at the bottom of the diagram. Additional rainfall along the course is indicated by thin curves, deposition of nucleus mass by thick curves. Solid curves are for 6 010 particles per cm³, broken for 1 200 per cm³, corresponding to 1.2×10^{-9} and 2.4×10^{-10} g/cm³, respectively. Hygroscopic/neutral mass is 1/5. The geometric mass mean radius is 10^{-4} cm, rainfall from above 2.5 mm/h and wind speed 5 m/s.

present on the diagram should of course have higher capacity for storing water than the lowest one, but a limit must eventually be reached.

4.4. *Wind force*

Results from two series of computations with systematic change in wind speed only are presented on Table 4 and Figs. 8 and 9.

When the wind is increased, less time is available at each unit of length along the course. This affects the condensation, and therefore the development of the droplet size distribution. A further effect is reduced removal of droplets of any specified size, resulting in a shift toward larger size in the droplet distribution and a higher liquid water content at any specified point in the course. It is seen from Table 4 that the final liquid water and nucleus mass contents increase with increasing wind.

Rainfall and deposition are measured per time unit at specified points along the course. Apart from the droplet size distribution, the local removals only depend on the immediate contents of the air. A stronger wind brings more air through the course, therefore more water and nucleus mass can be removed per time unit, and a total increase in extra rainfall and deposition should be expected.

The very first rainfall for the cases shown on Fig. 8 is highest for the weakest wind force. The reason is that the slower rate of condensation produces a droplet distribution with more droplets of such a large size that they can be removed. However, not much ascent is needed

Table 4. *Wind force effects*

Low hills: particle number 535 per cm³; particle geometric mass mean radius 4.65×10^{-5} cm. Rough terrain: particle number 6 010 per cm³; particle geometric mass mean radius 10^{-4} cm

Wind force (m/s)	Liquid water g/g dry air		Final fraction left of nuclei	
	Initial	Final	Mass	Number
Low hills				
1	6.46×10^{-7}	7.65×10^{-6}	0.07	0.86
2	6.46×10^{-7}	2.2×10^{-5}	0.12	0.87
5	6.46×10^{-7}	5.46×10^{-5}	0.33	0.90
Rough terrain				
2	1.33×10^{-5}	2.43×10^{-4}	0.06	0.87
5	1.33×10^{-5}	4.84×10^{-4}	0.13	0.90
10	1.33×10^{-5}	6.87×10^{-4}	0.35	0.93

before this effect is overtaken by the effect of increased transport through the course.

The feeder cloud precipitation at the forward brink of the first hill is only slightly influenced by the wind force. The removal of droplets in front of the hill is small even for the weakest wind force. The liquid water content is therefore close to the maximum value possible due to an ascent of 75 m. The extra rainfall cannot therefore increase much more with the wind force.

The influence is more pronounced further along the course. Even if the original liquid water contents are about similar, the air element with the highest speed looses the least droplets due to rain removal per unit length of the course. For a while the extra rainfall therefore becomes progressively higher.

Since less water has been removed from the air at a certain point for a strong than for a

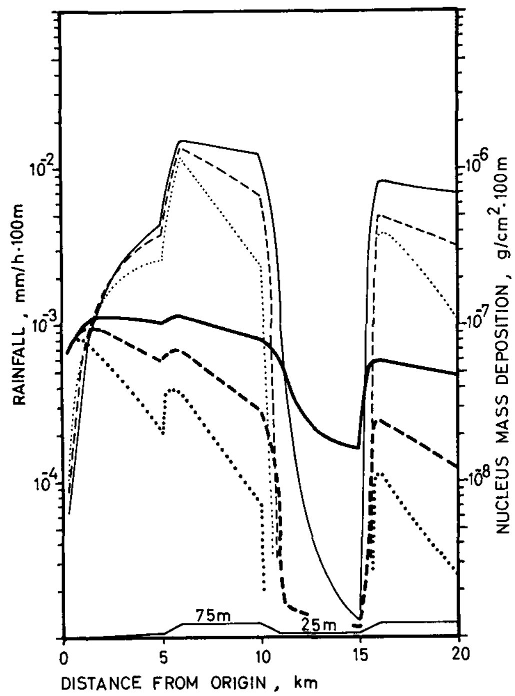

Fig. 8. Additional precipitation and deposition for different wind speeds. The course profile is shown at the bottom of the diagram. Additional rainfall along the course is indicated by thin curves, deposition of nucleus mass by thick curves. Dotted curves are for 1 m/s, broken for 2 m/s, and solid 5 m/s. The particle concentration is 535 per cm^3 with a geometric mass mean radius 4.67×10^{-5}, corresponding to 1.2×10^{-11} g/cm^3. Hygroscopic/neutral mass is 1/5. Rainfall from above is 1 mm/h.

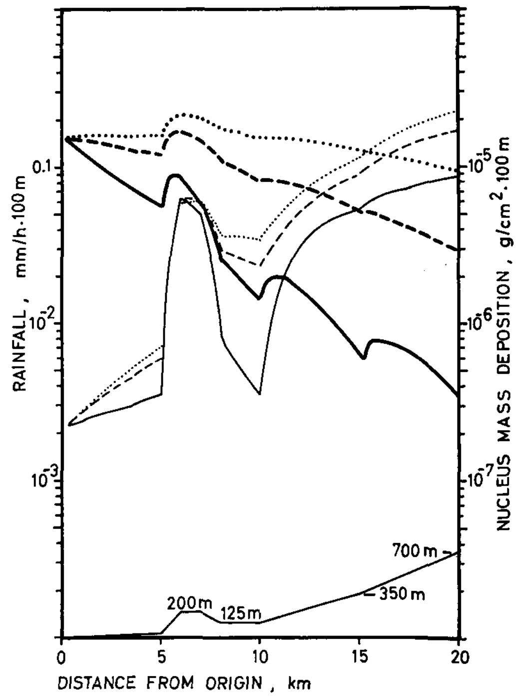

Fig. 9. Additional precipitation and deposition for different wind speeds. The course profile is shown at the bottom of the diagram. Additional rainfall along the course is indicated by thin curves, deposition of nucleus mass by thick curves. Solid curves are for 2 m/s, broken for 5 m/s and dotted for 10 m/s. The particle concentration is 6 010 per cm^3 with a geometric mass mean radius 10^{-4} cm, corresponding to 1.2×10^{-9} g/cm^3. Hygroscopic/neutral mass is 1/5. Rainfall from above is 2.5 mm/h.

weak wind, terrain effects may be more smoothed out for stronger winds. This is clearly seen from Fig. 8.

Mass deposition shows a similar pattern. The amount of material present in the air is independent of ascent or descent, and the deposition is all the time highest for the strongest winds.

Fig. 9 supports the conclusions drawn. The rainfall differences over the first short hill are small. At the forward brink a lower rainfall even is observed for the strongest wind. The condensation rate during ascent is here so high that the activation boundary is pushed towards quite small nucleus sizes, and much water is present on droplets so small that removal is low. After readjustment along the flat part of the hill, removal and extra precipitation pick up.

Table 5. *Effects of rainfall from above*

Low hills: particle number 3 770 per cm³; particle geometric mass mean radius 4.65×10^{-5} cm. Rough terrain: particle number 1 200 per cm³; particle geometric mass mean radius 10^{-4} cm

Rainfall from above (mm/h)	Liquid water g/g dry air		Final fraction left of nuclei	
	Initial	Final	Mass	Number
Low hills				
0.5	2.67×10^{-6}	7.4×10^{-5}	0.60	0.99
1	2.67×10^{-6}	5.84×10^{-5}	0.45	0.98
2	2.67×10^{-6}	3.91×10^{-5}	0.31	0.96
Rough terrain				
1	5.45×10^{-6}	6.62×10^{-4}	0.24	0.84
2.5	5.45×10^{-6}	4.45×10^{-4}	0.06	0.74

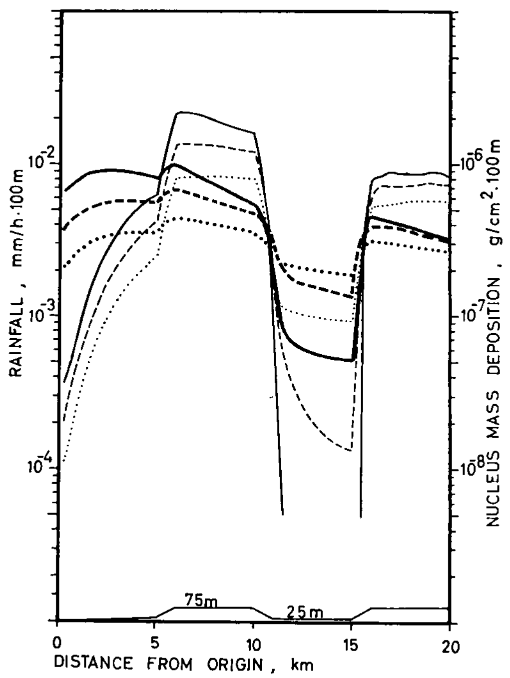

Fig. 10. Additional precipitation and deposition for different rainfalls from above. The course profile is shown at the bottom of the diagram. Additional rainfall along the course is indicated by thin curves, deposition of nucleus mass by thick curves. Dotted curves are for a rainfall of 0.5 mm/h, broken for 1 mm/h and solid for 2 mm/h. The particle concentration is 3 770 per cm³, with a geometric mass mean radius 4.64×10^{-5}, corresponding to 8.46×10^{-11} g/cm³. Hygroscopic/neutral mass is 1/5. Wind speed is 5 m/s.

The effect of the wind is more apparent over the lower intermediate part of the course in this diagram than in the previous. As should be expected because of a limited liquid water storage capacity of the air, the rainfall differences are greater during the final ascent than over the first hill.

The deposition curves may be even more influenced by the wind. A number of features which are well developed for weak wind forces, are merely slight inflections on the curve for 10 m/s.

4.5. *Rainfall from above*

Results from two series of computations with a systematic change in rainfall from above are presented in Table 5 and Figs. 10 and 11.

The effect of increased rainfall is to remove more of the droplets present, and Table 5 shows that nucleus masses left and final liquid water contents are decreased.

Because the liquid water storage capacity in the air has its limits, first order effects due to differences in absolute removal should only be present for the first part of the course. The droplet size distributions are changed due to different removal rates. A further modification takes place by evaporation and condensation processes, and a sort of balance should be achieved between content and removal of the liquid water.

The course in Fig. 10 is not long enough for this to occur over the hills, but both rainfall and deposition curves are finally closer together than initially. Over the lower part of the course

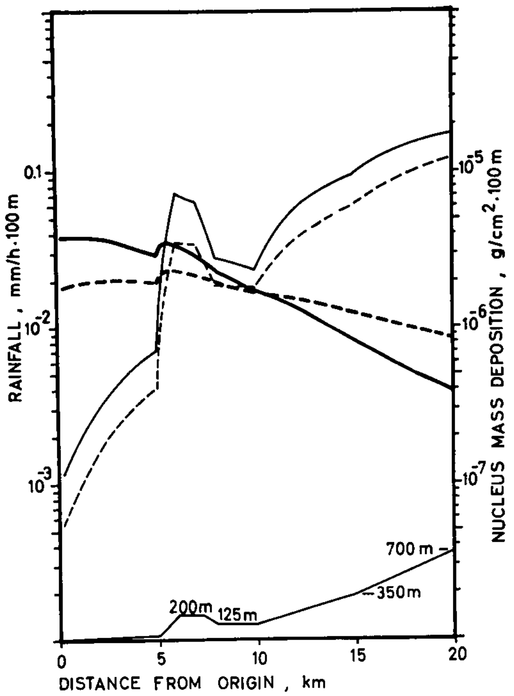

Fig. 11. Additional precipitation and deposition for different rainfalls from above. The course profile is shown at the bottom of the diagram. Additional rainfall along the course is indicated by thin curves, deposition of nucleus mass by thick curves. Broken curves are for a rainfall of 1 mm/h, solid for 2.5 mm/h. The particle concentration is 1 200 per cm^3, with a geometric mass mean radius 10^{-4} cm, corresponding to 1.2×10^{-9} g/cm^3. Hygroscopic/neutral mass is 1/5. Wind speed is 5 m/s.

the positions of the curves are reversed, because evaporation and droplet sizes after descent are sensitive to removal earlier along the course. It might be of interest to note that the increase in extra rainfall, even over the first hill, is less than proportional to the increase in rainfall from above.

A first impression from Fig. 11 is increased extra rainfall everywhere with increased rainfall from above. The effect of the higher rate of liquid water depletion is, however, seen in decreasing rainfall along the horizontal ranges of the course. The extra rainfall, even over the first hill, is less than proportional to the increase in rainfall from above.

The removal of nuclei is considerably greater for the rough terrain course than for the low hills course. The effect is a reversed position for the mass deposition curves about midway along the course.

5. Discussion and conclusions

The intent of this paper is to discuss the influence on rainfall patterns of droplet removal in low air layers due to raindrops falling from above. Since this problem might be linked closely to the condensation nuclei present, the influence of the nuclei themselves has been studied. It appears quite clearly that neither nucleus composition, mean size nor number concentration have any marked influence on the precipitation pattern.

Division of a supposedly continuous nucleus distribution into classes is a weakness of the procedures used. This should, however, partly be overcome by computation of the droplet development for different distributions and different course profiles. From the composite data a certain conception of the condensation development is formed.

For low relative humidities the hygroscopic nuclei attract enough water to be close to stable equilibrium with the air humidity, i.e. they are inactive. With increasing relative humidity a number of the nuclei are activated, i.e. they become instable with regard to their droplet saturation humidity. Activated nuclei can never form a stable system, since droplets with a saturation humidity lower than the immediate value in the air must grow, while the rest must evaporate. A continuous adjustment of the activated droplet assembly thus occurs, in general leading to fewer but larger droplets when no cooling or heating of the air occurs.

When the rate of cooling increases, more nuclei may be activated. If the droplets already present cannot keep the relative humidity low enough, the best of the inactive nuclei become activated. But this process stops at the moment enough droplets are present to cope with the situation. This is the reason why composition, size or number of the nuclei play a minor role. These characteristics are only important for their ability to store water in non-activated state. Minor effects due to the distribution density of nuclei in the boundary region are, of course, not excluded.

But the effect of overseeding a cloud in order to avoid precipitation is certainly doubtful, at least if time enough is available for the droplet size distribution to be adjusted. But for short condensation spells or violent changes in state, the more subtle effects of interaction between the various droplets due to condensation and evaporation may be submerged.

If the air is cooled quickly, more nuclei are activated than necessary for a slower cooling. A subsequent change to a lower rate will lead to adjustments. The air humidity will seek to take on a value within the range of the saturation humidities for the droplets present. Since the droplet saturation humidity normally decreases with increasing size in the activated part of the distribution, the smallest droplets thereby evaporate.

The condensation concept described eliminates the nucleus itself as an important parameter, as long as a sufficient number of nuclei are present. The nucleus number is not reduced to a critical level for any of the cases presented.

All the cases studied for the low hills course indicate that the rainfall is increased over the hills. Conclusions regarding natural conditions may with caution be drawn from the computer model.

It should be taken into consideration that woods often grow on the hills while the lowland inbetween are pastures. This could cause greater vertical displacements of the air than those of the topography. In addition a real hill may have a form more suitable for a peaked maximum than the courses studied. The computer model requires a feeder cloud thickness of 1 000 m in order to increase the rainfall by some 10 per cent. Natural conditions may lead to a reduced requirement. The study thus seems to support the explanation Bergeron has given to his measurements.

It should be emphasized that the computations are limited to steady state conditions. They are not directly valid for the normal situation where both rainfall from above and ground flow are variable. Further no correction is made in raindrop size distribution due to the removal, which may be important for a thick cloud.

The distributions of rainfall and radioactivity in the Samnanger area have earlier been explained by the present author (Storebø, 1968) as being due to droplet removal below a precipitating cloud. The plausibility of such a hypothesis may be quantitatively discussed in connection with Fig. 9, since the rough course profile is meant to represent the conditions in the Samnanger fjord and valley area in Western Norway.

The rainfall measurements in question were 2.5 m per year for a station on the frontside of the small hill, and 3.1 m for a station at about 400 m height. The radioactivity, which is associated with particles, shows deposition at the second station of about 0.6 of that at the first.

If the 5 m/s curves in Fig. 9 are used, the first station gets an extra rainfall of 2.5×10^{-2} and the second 0.1 mm/h·100 m. The rainfall from above is 2.5 mm/h, and an air layer 6–700 m deep would produce the desired ratio between total precipitation at the two stations. The nucleus mass deposition ratio is 0.32, much lower than the radioactivity ratio measured.

Even when the uncertainties regarding air layer depth, wind force, rainfall rate or radioactivity size distribution are taken into account, the measured results are well within the limits indicated by the computation of droplet removal.

However, if this explanation is correct, a total rise of 700 m for the low level air is necessary, because the valley sides prevent escape of air at lower heights. This is at odds with the measurement series of radioactive deposition and air concentration at Bergen and at Finse, where the radioactivity data at both positions indicated a mean rise of the feeder clouds of less than 300 m.

However, it is possible that different zones of western Norway are involved here. Moving from west to east, Bergen is in front of the valley system. The surroundings are rough terrain, but channels are available for the air flow in any direction. Samnanger is in the valley system, where the air is channelled in a west–east direction. Finse is well behind the valley system, on a mountain field where no unidirectional channelling occurs.

Precipitation areas moving in from the west normally undergo some general strengthening when the air is forced against the mountain ridge. In addition the lower air layers are set in motion and some lifting occurs. The heavy terrain-induced friction in front of the valley system causes a general drift towards lower pressure, i.e. crossing the general wind and the direction of movement of the precipitation area.

It is therefore well possible that these air masses only take part in the precipitation formation as low feeder clouds, where droplets and impurities are removed by the raindrops falling from above. The bulk of the low layer air does not penetrate much inland and is soon bygone by the overlying precipitation area.

In the valley system further inland the low level air cannot easily drift, since it is bound to follow the valley which may have sides going up to 700–1 000 m height. The valley bottoms gradually rise to the same height. A considerable ascent will therefore occur, and a greater fraction of water and nuclei are removed. Small scale changes in slope, small hills and bottlenecks for the further flow at low level should then be reflected in the rainfall pattern in manners and degrees analogous to those illustrated for the rough terrain course.

On the mountain field ground level air may again drift more freely, and a situation similar to that at Bergen may therefore be established at Finse.

The computations presented indicate that many small scale influences of topographic features on the rainfall pattern during passages of extensive precipitation systems, may be due to droplet removal from fairly independent underlying clouds. Although only steady state problems are examined, it is believed to be the most important mechanism by which small scale topographic features impress themselves on the precipitation pattern.

REFERENCES

Bergeron, T. 1949. The problem of artificial control of rainfall on the globe. II. The coastal orographic maxima of precipitation in autumn and winter. *Tellus 1*, no. 3, 15–32.

Bergeron, T. 1950. Über den Mechanismus der ausgiebigen Niederschläge. *Berichte des Deutschen Wetterdienstes in der US-Zone*, no. 12, pp. 225–232.

Bergeron, T. 1960. Operation and results of "Project Pluvius". In *Physics of precipitation*, Geophysical Monograph no. 5, Washington D.C., American Geophysical Union, pp. 152–157.

Bergeron, T. 1965. On the low-level redistribution of atmospheric water caused by orography. *Proc. Int. Conf. on Cloud Physics, Tokyo and Sapporo*, 1965.

Bergeron, T. 1967–1973. *Mesometeorological studies of precipitation*, vol. I–V. Meteorologiska Institutionen, Uppsala.

Fuchs, N. A. 1959. *Evaporation and droplet growth in gaseous media.* Pergamon Press, London, Oxford, New York and Paris.

Goff, J. A. & Gratch, S. 1946. Low-pressure properties of water from − 160 to 212 F, *Trans. Amer. Soc. Heat. Vent. Eng. 52*, 95–121.

Hodgman, C. D. 1961. *Handbook of chemistry and physics.* The Chemical Rubber Publishing Co., Cleveland.

Low, R. D. H. 1969. A generalized equation for the solution effect in droplet growth. *J. appl. Meteor. 26*, 608–611.

Marshall, J. S. & McK Palmer, W. 1948. The distribution of raindrops with size. *J. Meteor. 5*, 165.

Mason, B. J. 1971. *The physics of clouds*, 2nd ed. Clarendon Press, Oxford.

Squires, P. 1952. The growth of cloud droplets by condensation. I. General characteristics. *Aust. J. Sci. Res. A 5*, 59.

Storebø, P. B. 1968. Precipitation formation in a mountainous coast region. *Tellus 20*, 239–250.

Storebø, P. B. & Dingle, A. N. 1974. Removal of pollution by rain in a shallow air flow. *J. Atm. Sci. 31*, 533–542.

ВЛИЯНИЕ МЕЛКОМАСШТАБНОЙ ТОПОГРАФИИ НА ОСАДКИ

Когда влажный воздух дует над ландшафтом, то над невысокими холмами могут образовываться небольшие облака. Удаление капелек из этих облаков каплями дождя сверху над ними является единственным предложенным механизмом, прямо связывающим места выпадений дождя с мелкомасштабными топографическими особенностями. Этот механизм исследуется теоретически и представлены результаты ряда вычислений. Найдено, что свойства ядер конденсации не имеют большого значения для развития процесса конденсации, потому что активация ядер прекращается, когда уже сформировано достаточное количество капель, и потому, что ансамбль капелек является неустойчивым. Найдено, что дополнительное выпадение дождя над небольшими холмами является достаточно заметным для объяснения наблюдаемого влияния мелкомасштабных особенностей топографии на осадки в Скандинавии.